Stable Solid-State Source of Single Photons

Christian Kurtsiefer,[1] Sonja Mayer,[1] Patrick Zarda,[2] and Harald Weinfurter[1,2]
[1]*Sektion Physik, Ludwig-Maximilians-Universität, D-80799 München, Germany*
[2]*Max-Planck-Insitut für Quantenoptik, D-85748 Garching, Germany*
(Received 27 March 2000)

Fluorescence light observed from a single nitrogen-vacancy center in diamond exhibits strong photon antibunching: The measured pair correlation function $g^{(2)}(0)$ shows that only one photon is emitted at a time. Nitrogen-vacancy centers are well localized, stable against photobleaching even at room temperature, and can be addressed in simple experimental configurations.

PACS numbers: 42.50.Dv, 78.55.–m

The generation of nonclassical light and particularly of single photon states is one of the crucial experimental tasks in quantum optics. The ideal single photon source emits light such that only one of two detectors behind a semitransparent beam splitter registers an event. A specially suited process for that is fluorescence of a single two-level quantum system. Since excitation and subsequent decay to the initial state takes a finite time, only one photon is emitted at a time.

Such two-level systems can be found with good approximation in atoms and ions, where, after initial demonstrations [1], experiments now concentrate on increasing the yield and the rate of single photons [2]. While manipulation of single trapped atoms or ions still requires significant technical effort, single organic dye molecules as the fluorescent emitter in solvents or polymers allow much simpler setups [3,4]. Despite recently reported progress [5], organic molecules still degrade rapidly at room temperature—typically after about 10^9 emissions. Thus, these systems seem impractical for applications requiring single photon sources, i.e., quantum cryptography, where perfect security is given only for single photon pulses [6].

Here, we present an alternative candidate for generating single photons. Single nitrogen-vacancy (NV) centers in diamond combine the robustness of single atoms with the simplicity of experiments with dye molecules.

NV centers are one of many well studied luminescent defects in diamond [7–10]; they are formed by a substitutional nitrogen atom with a vacancy trapped at an adjacent lattice position. Usually, these centers are prepared in type Ib synthetic diamond, where single substitutional nitrogen impurities are homogeneously dispersed. To observe bright luminescence from a sample, additional vacancies are created by electron or neutron irradiation [10,11], and allowed to diffuse to the nitrogen atoms by annealing at 900 °C. However, it turned out that already untreated samples of synthetic Ib diamond provide a concentration of NV centers well suited for addressing *individual* centers. The high radiative quantum efficiency even at room temperature of close to one as well as a short decay time of the excited state [12] makes them well-suited for single photon generation.

Our experimental setup is shown in Fig. 1. Diamond samples of $500 \times 500 \times 250$ μm were illuminated by the light of a diode pumped frequency doubled Nd:YVO_4 laser at a wavelength of $\lambda = 532$ nm. The light was focused into the diamond with a relay lens and a standard microscope objective of magnification 60 and a numerical aperture of 0.85 to a spot size of 430 nm inside the diamond. The fluorescence light was extracted with the same microscope objective, and focused into a single mode optical fiber. The fiber defines the spatial mode for confocal detection, with the corresponding acceptance area in the diamond sample having a FWHM diameter of 1.6 μm. To suppress coupling of pump light into the fluorescence detection setup, we used a combination of a dichroic mirror and a color glass filter.

A piezoelectric two-dimensional scanning unit was used to move the diamond probe transversely to the optical axis, and a motorized linear translation stage to choose the longitudinal position of the focal spot within the diamond. The fluorescence light from the single NV center was analyzed either by a Hanbury-Brown–Twiss configuration or a grating spectrometer. Finally, it was detected by passively quenched silicon avalanche photodiodes (APD) with a dark count rate of ≈250 counts per second (cps). The

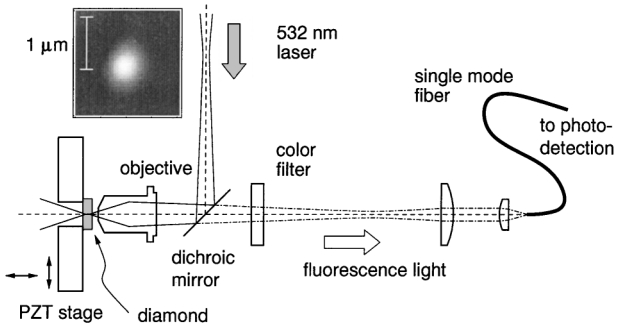

FIG. 1. Experimental setup: A frequency doubled diode pumped solid-state laser (532 nm) is focused into a type Ib diamond crystal. Fluorescence light is collected with a confocal microscope into a single mode optical fiber, and detected with silicon APDs. The inset shows the fluorescence image of a single NV center.

 0031-9007/00/85(2)/290(4)$15.00

total detection efficiency for our setup was approximately 1.5×10^{-4}.

The inset of Fig. 1 shows the image of a single NV center. The transverse width of 470 nm corresponds to the size of the calculated laser waist in the diamond. In longitudinal direction, we observe a 2.6 μm (FWHM) wide acceptance region for fluorescence light detection. Within a volume of $15 \times 15 \times 64$ μm, we found 72 localized luminescence centers resulting in a density of about 5×10^9 cm^{-3} in an untreated type Ib diamond sample. Radiation damage in the crystal by exposing diamond samples to fast neutrons and/or heat treatment increased that density, but for investigating single luminescence centers, the untreated samples were sufficient.

Spectral analysis allowed us to clearly identify the single NV centers (Fig. 2a). Even at room temperature the zero phonon line at 637 nm is clearly visible, and additional phonon contributions result in the characteristic spectral shape with an overall width of about 120 nm [7,8]. This broad spectral emission is one of the few drawbacks of NV center fluorescence. For applications it will be mandatory to increase the spectral yield in narrow wavelength bands, most likely by using microcavities [4].

For our excitation wavelength of 532 nm, we observed one- and two-phonon Raman scattering contributions from bulk diamond at 573 nm and between 600 and 620 nm, respectively. For all other measurements, we suppressed that light with an additional optical band pass filter (RF, inset of Fig. 3).

The luminescence from a single NV center placed in the beam waist of the excitation laser shows a clear saturation behavior; in Fig. 2b, the recorded fluorescence on and beside a NV center is shown as a function of pump power. While the background increases linearly with power, the fluorescence contribution has a power dependence of the form $F = F_0 P/(P_{\mathrm{sat}} + P)$, with $P_{\mathrm{sat}} = 1.3$ mW corresponding to a saturation intensity of $I_{\mathrm{sat}} = 3.6 \times 10^9$ W m^{-2}.

Because of the immobility of the vacancy and the substitutional nitrogen atom, NV centers are very stable. All measurements presented here were performed on the same NV center. Even after more than a week of operation corresponding to $\approx 10^{13}$ emission events, we did not observe any changes in the emission characteristics.

To demonstrate the nonclassical properties of the fluorescence from single NV centers, the second order correlation function $g^{(2)}(\tau)$ was measured for different excitation

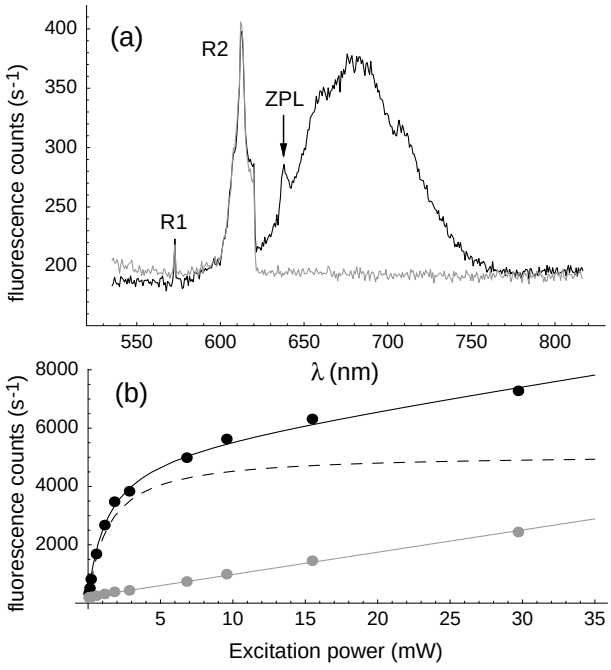

FIG. 2. (a) Fluorescence spectrum of a single NV center (black) and reference spectrum from an empty region in type Ib diamond (gray). Besides the zero phonon line (ZPL) at $\lambda = 637$ nm and the vibrationally broadened spectrum of the NV center, single- (R1) and two-phonon Raman scattering (R2) from crystalline diamond occurs. (b) Fluorescence as a function of the excitation power from a single NV center (black) and from bulk diamond (grey). The background contribution increases linearly with intensity, while the NV contribution (dashed) saturates, with a saturation power of 1.32 mW. (Error bars are smaller than symbols.)

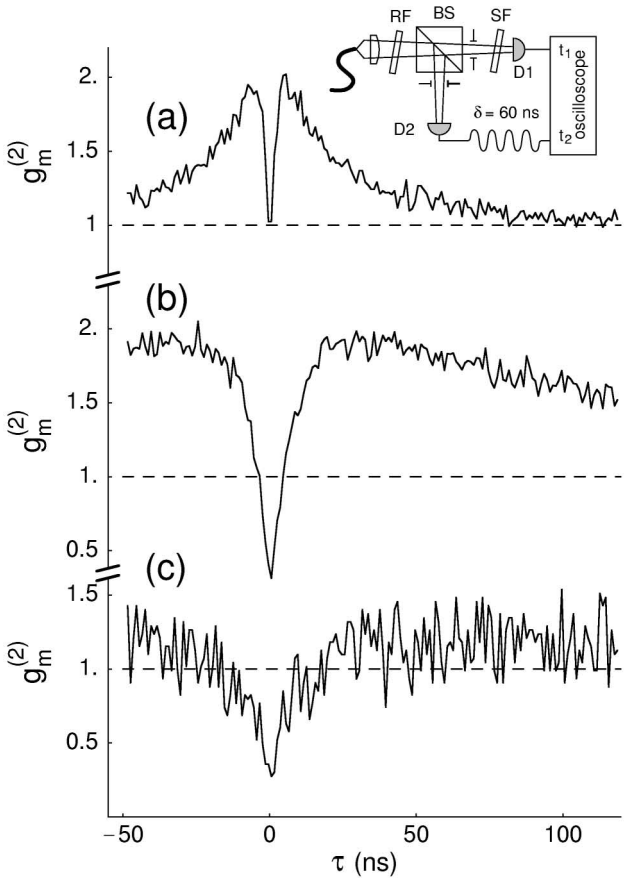

FIG. 3. Measured pair correlation function $g_m^{(2)}(\tau)$: fluorescence light is sent through a beam splitter BS and two filters RF, SF onto two photodiodes D1, D2, to record detection time difference $\tau = t_2 - t_1$. The normalized histograms of $t_2 - t_1$ for excitation powers of (a) $0.16P_{\mathrm{sat}}$, (b) $1.6P_{\mathrm{sat}}$, and (c) $30P_{\mathrm{sat}}$ show a clear signature of photon antibunching around $\tau = 0$.

powers with two APDs behind a beam splitter (BS, inset of Fig. 3). To suppress cross talk due to light created by a detection event of the other detector we inserted a filter (SF) blocking that fluorescence above 750 nm. The differences of detection times $\tau = t_2 - t_1$ of photon pair events, shifted by a transmission line delay of $\delta = 60$ ns for technical reasons, were recorded in a storage oscilloscope with a conditional trigger mode. Timing jitter in the APDs and electronics was determined independently to lead to a spreading of τ with a FWHM of 1.4 ns.

A normalized distribution of time differences τ is equivalent to $g^{(2)}(\tau)$ as long as τ is much smaller than the mean time between detection events [13]. To obtain the measured correlation function $g_m^{(2)}(\tau)$ from a delay time histogram, we divide the number of entries in each time bin by $r_1 \times r_2 \times t_{\text{bin}} \times T_{\text{int}}$, where r_1 and r_2 are the mean count rates per second, t_{bin} the time bin width, and T_{int} the total integration time.

Figures 3a–3c exemplarily show $g_m^{(2)}(\tau)$ for different excitation powers. Most prominently, the minimum at zero delay clearly proves the nonclassical character of the emitted fluorescence. However, due to residual background and timing jitter this minimum does not vanish completely. We obtain a minimum value $g_m^{(2)}(\tau = 0) = 0.26$ for a pump power of 5 mW; within our experimental errors, this is compatible with perfect photon antibunching, taking into account the background count rate contribution of 12% for that experiment. With increasing τ, the antibunching signature in $g_m^{(2)}(\tau)$ decays exponentially. We also observe an increase of $g_m^{(2)}$ above 1, which becomes more prominent with increasing excitation power ($0.16P_{\text{sat}}$ in Fig. 3c to $1.6P_{\text{sat}}$ in Fig. 3b). For extremely high excitation power ($30P_{\text{sat}}$ in Fig. 3a), the excess in the photon correlation relaxes rapidly to the Poisson-like statistics for very large τ.

Such results are not compatible with a simple two-level model. From hole-burning effects at low temperatures it is known that there exists a metastable shelving state [9,14] (Fig. 4a). This state is thermally coupled to the excited state and at low temperatures, repumping is necessary to depopulate it to observe higher fluorescence rates [15]. At room temperature, the thermal coupling between the shelving and the excited state becomes very strong, and shelving was assumed to be of no significance anymore. However, as becomes apparent from our experiments, on very short time scales the presence of the shelving state still influences the emission probability of single photons.

The dependence of the correlation function on the excitation power can be described with a rate equation for the three-level model. Neglecting all coherences, the population dynamics is governed by

$$\begin{pmatrix} \dot{\varrho}_1 \\ \dot{\varrho}_2 \\ \dot{\varrho}_3 \end{pmatrix} = \begin{pmatrix} -k_{12} & k_{21} & 0 \\ k_{12} & -k_{21} - k_{23} & k_{32} \\ 0 & k_{23} & -k_{32} \end{pmatrix} \cdot \begin{pmatrix} \varrho_1 \\ \varrho_2 \\ \varrho_3 \end{pmatrix}, \tag{1}$$

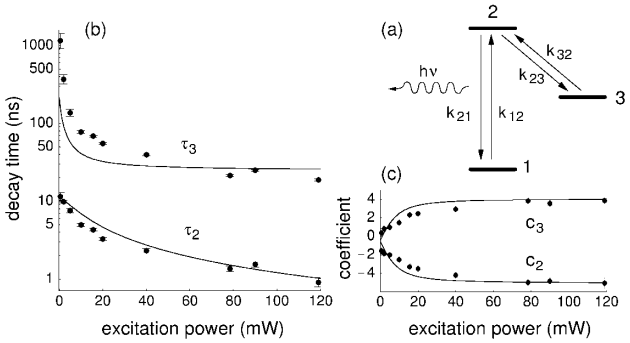

FIG. 4. (a) Three-level model for the fluorescence from the NV center. The excitation is described by a pump rate coefficient k_{12}, fluorescent decay by a coefficient k_{21} and coupling with a shelving state by coefficients k_{23} and k_{32}, respectively. (b) Decay times $\tau_{2,3}$ and (c) coefficients $c_{2,3}$ for various excitation powers, obtained from a least squares fit to data shown in Fig. 3 with the model given in Eq. (2). The solid lines show the power dependence given by Eq. (3) for $1/k_{21} = 20.1$ ns, $1/k_{23} = 31$ ns, and $1/k_{32} = 127$ ns. The proportionality constant between k_{12} and excitation power is obtained from the observed saturation power P_{sat} and Eq. (4).

with the initial condition $\varrho_1 = 1$, $\varrho_2 = \varrho_3 = 0$ for the system being prepared in the ground state 1 by a fluorescence decay. Here we neglect possible nonradiative transitions from the shelving state 3 to the ground state, which are about 3 orders of magnitude smaller than all other rates [15]. The instantaneous emission probability of a photon is then proportional to $\varrho_2(t)$, and an analytical expression for the second order correlation function is obtained by normalizing $\varrho_2(t)$ to $\varrho_2(t \to \infty)$ resulting in

$$g^{(2)}(\tau) = 1 + c_2 e^{-\tau/\tau_2} + c_3 e^{-\tau/\tau_3}, \tag{2}$$

where the decay times and coefficients are given by

$$\tau_{2,3} = 2/(A \pm \sqrt{A^2 - 4B})$$
$$c_2 = \frac{(1 - \tau_2 k_{32})}{k_{32}(\tau_2 - \tau_3)}, \qquad c_3 = -1 - c_2 \tag{3}$$

with

$$A = k_{12} + k_{21} + k_{32} + k_{23},$$
$$B = k_{12}k_{23} + k_{12}k_{32} + k_{21}k_{32}.$$

With these abbreviations, the steady-state population of level 2 is given by

$$\varrho_2(t \to \infty) = k_{23}k_{12}/B, \tag{4}$$

showing a saturation behavior as a function of the pump rate k_{12}.

To link our experimental results with the outcome of the model, it is necessary to correct for background contributions. Coefficients $\tilde{c}_{2,3}$ and $\tau_{2,3}$ are obtained from

a least squares fit of Eq. (2) with measured correlation functions $g_m^{(2)}(\tau)$ (Fig. 3) for a given excitation power P. With the probability p_f that an observed photo event is due to an emission event from the NV center (known from the saturation behavior), the actual coefficients are given by $c_{2,3}(P) = \tilde{c}_{2,3}(P)/p_f(P)^2$. Their values and the decay times $\tau_{2,3}$ are shown for a set of pump powers in Fig. 4. First estimates for the model coefficients in Eq. (1) can be deduced from the limiting cases for high or low pump intensities from asymptotical solutions for the coefficients:

$$k_{32} = 1/(1 + c_3^{(\infty)}\tau_3^{(\infty)}), \qquad k_{23} = c_3^{(\infty)}k_{32}\,,$$
$$k_{21} = \frac{1}{\tau_2^{(0)}} - \frac{k_{32}}{1 - \tau_2^{(0)}k_{32}}\,, \tag{5}$$

where $\tau_2^{(0)} = \tau_2(P \to 0)$, etc.

For the least squares fit of the data the long decay times τ_3 should not be considered, since the correlation data are collected over an interval of only 120 ns. On the other hand, the short values for τ_2 are already influenced by the timing jitter of our detectors and should also be disregarded. For small pump power the decay time τ_2 converges to $\tau_2^{(0)} = 11.7 \pm 0.3$ ns. This is in good agreement with a decay time of 11.6 ns measured in a pulsed excitation experiment [12]. The high power limits of $c_{2,3}$ determine the ratio $k_{23}/k_{32} = 4.1 \pm 0.1$. Finally, we are led to the room temperature rate coefficients $1/k_{21} = 20.1 \pm 1.6$ ns, $1/k_{23} = 31 \pm 2.5$ ns, and $1/k_{32} = 127 \pm 11$ ns.

In summary, the fluorescence of NV centers in synthetic Ib diamond shows clear signatures of nonclassical light. The emission spectrum lies in the conveniently detectable red to near infrared region, decay times are short, and the radiative quantum efficiency is close to one. For short times τ, we observed strong photon antibunching, making this system a prime candidate for single photon generation by pulsed excitation. For this purpose, the significant influence of a shelving state requires the pulse rate at room temperature to stay below 5 MHz in order to avoid population buildup at intermediate times. Foremost, it is the robustness against photobleaching and the simplicity of the all-solid-state setup which distinguishes NV centers from other fluorescing quantum systems. The potential for miniaturizing the setup and the superior stability makes NV centers very attractive both for practical single photon sources and cavity-QED measurements in experimentally simple environments.

We acknowledge helpful discussions with J. Wrachtrup and the uncomplicated help of H. Gerstenberg for neutron irradiation of the first samples. This work was supported by the Deutsche Forschungsgemeinschaft (Project No. WE2451/1) and the ESPRIT Project EQUSPOT (EC28139).

[1] H. J. Kimble, M. Dagenais, and L. Mandel, Phys. Rev. Lett. **39**, 691 (1977); F. Diedrich and H. Walther, Phys. Rev. Lett. **58**, 203 (1987).
[2] A. Kuhn, M. Hennrich, T. Bondo, and G. Rempe, Appl. Phys. B **69**, 373 (1999).
[3] W. E. Moerner and L. Kador, Phys. Rev. Lett. **62**, 2535 (1989); M. Orrit and J. Bernard, Phys. Rev. Lett. **65**, 2716 (1990); T. Plakhotnik, E. Donley, and U. P. Wild, Annu. Rev. Phys. Chem. **48**, 181 (1997).
[4] F. De Martini, G. Di Giuseppe, and M. Marrocco, Phys. Rev. Lett. **76**, 900 (1996); S. C. Kitson, P. Jonsson, J. G. Rarity, and P. R. Tapster, Phys. Rev. A **58**, 620 (1998).
[5] X. S. Xie and J. K. Trautmann, Annu. Rev. Phys. Chem. **49**, 441 (1998); C. Brunel, B. Lounis, P. Tamarat, and M. Orrit, Phys. Rev. Lett. **83**, 2722 (1999); L. Fleury, J.-M. Segura, G. Zumofen, B. Hecht, and U. P. Wild, Phys. Rev. Lett. **84**, 1148 (2000).
[6] The commonly used weak laser pulses have a certain probability to contain more than one photon at a time, and thus do not ensure perfect security in quantum cryptography: G. Brassard, N. Lütgenhaus, T. Mor, and B. C. Sanders, quant-ph/9911054.
[7] *The Properties of Natural and Synthetic Diamond*, edited by J. E. Field (Academic Press, London, 1992).
[8] A. Gruber, A. Dräbenstedt, C. Tietz, L. Fleury, J. Wrachtrup, and C. von Borczyskowski, Science **276**, 2012 (1997).
[9] R. T. Harley, M. J. Henderson, and R. M. Macfarlane, J. Phys. C **17**, L233 (1984).
[10] G. Davies and M. F. Hamer, Proc. R. Soc. London A **348**, 285–298 (1976).
[11] H. Hanzawa *et al.*, Phys. Rev. B **54**, 3793 (1996).
[12] A. T. Collins, M. F. Thomaz, and M. I. B. Jorge, J. Phys. C **16**, 2177 (1983).
[13] S. Reynaud, Ann. Phys. (Paris) **8**, 351 (1983).
[14] N. R. S. Reddy, N. B. Manson, and E. R. Krausz, J. Lumin. **38**, 46 (1987).
[15] A. Dräbenstedt, Ph.D. thesis, University of Jena, 1999.